

Strain-Promoted Catalyst-Free Click Chemistry for Rapid Construction of ^{64}Cu -Labeled PET Imaging Probes

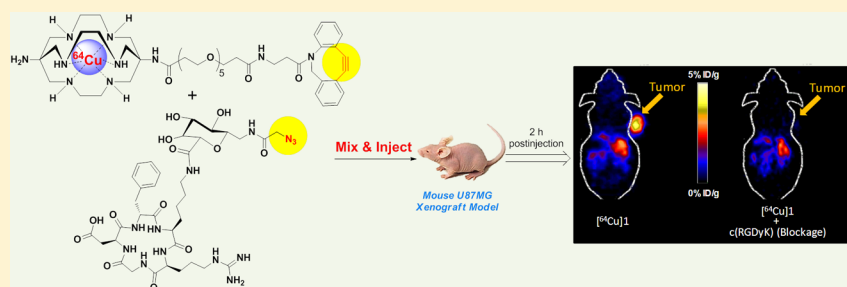
Kai Chen,^{*,†} Xinlu Wang,^{†,||,§} Wei-Yu Lin,^{‡,§} Clifton K.-F. Shen,[‡] Li-Peng Yap,[†] Lindsey D. Hughes,[†] and Peter S. Conti^{*,†}

[†]Molecular Imaging Center, Department of Radiology, Keck School of Medicine, University of Southern California, Los Angeles, California 90033, United States

[‡]Department of Molecular and Medical Pharmacology, University of California at Los Angeles, Los Angeles, California 90095, United States

^{||}Department of Nuclear Medicine and PET-CT Center, Guangzhou General Hospital of Guangzhou Military Command, Guangzhou 510010, China

S Supporting Information



ABSTRACT: A rapid, efficient, and catalyst-free click chemistry method for the construction of ^{64}Cu -labeled PET imaging probes was reported based on the strain-promoted aza-dibenzocyclooctyne ligation. This new method was exemplified in the synthesis of ^{64}Cu -labeled RGD peptide for PET imaging of tumor integrin $\alpha_v\beta_3$ expression *in vivo*. The catalyst-free click chemistry reaction proceeded with a fast rate and eliminated the contamination problem of the catalyst Cu(I) ions interfering with the ^{64}Cu radiolabeling procedure under the conventional Cu-catalyzed 1,3-dipolar cycloaddition condition. The new strategy is simple and robust, and the resultant ^{64}Cu -labeled RGD probe was obtained in an excellent yield and high specific activity. PET imaging and biodistribution studies revealed significant, specific uptake of the “click” ^{64}Cu -labeled RGD probe in integrin $\alpha_v\beta_3$ -positive U87MG xenografts with little uptake in nontarget tissues. This new approach is versatile, which warrants a wide range of applications for highly diverse radiometalated bioconjugates for radioimaging and radiotherapy.

KEYWORDS: PET imaging probe, ^{64}Cu radiolabeling, catalyst-free click chemistry, integrin $\alpha_v\beta_3$, *in vivo*

Positron emission tomography (PET) is a nuclear imaging technique used to map biological and physiological processes in living subjects.^{1–3} Unlike morphological imaging techniques, such as computed tomography (CT), PET requires the injection of molecular probes in a tested subject in order to acquire the imaging signal from molecular probes labeled with positron-emitting radionuclides.^{4,5} Fluorine-18 and carbon-11 are two conventional PET radionuclides used for the development of PET imaging probes. Due to the short half-lives of fluorine-18 (109.8 min) and carbon-11 (20.3 min), ^{18}F - or ^{11}C -labeled PET probes must be radiosynthesized with the need for an on-site cyclotron, and the PET imaging of a subject using ^{18}F - or ^{11}C -labeled PET probes must be performed within a few hours.⁶ In addition to ^{18}F and ^{11}C , several nonconventional metallic radionuclides, such as ^{64}Cu , ^{68}Ga , ^{86}Y , and ^{89}Zr , have been applied to PET probes.⁷ These metallic PET isotopes are usually characterized by longer half-lives, allowing the evaluation of radiopharmaceutical kinetics in the

same subject to be achieved by successful PET imaging over several hours or even days. Among these metallic radionuclides, ^{64}Cu ($t_{1/2} = 12.7$ h; β^+ 655 keV, 17.8%) has attracted considerable interest because of its favorable decay half-life, low β^+ energy, and commercial availability.^{8–10} As the half-life of ^{64}Cu is relatively short, fast, clean, and reliable chemistry which can proceed efficiently under mild condition is required for ^{64}Cu labeling of biomolecules. The exploration of new ^{64}Cu -labeling methods using a simple, versatile, and modular approach is thus highly demanded.

Click chemistry offers chemists a platform for general, modular, and high yielding synthetic transformations for constructing highly diverse molecules.¹¹ The Huisgen 1,3-dipolar cycloaddition reaction, which fuses an azide and an

Received: August 10, 2012

Accepted: September 19, 2012

Published: September 19, 2012

alkyne together, and provides access to a variety of five-membered heterocycles, has become of great use in labeling studies, in the development of new therapeutics and nanoparticles, and in protein modification.^{12–15} However, the Huisgen 1,3-dipolar cycloaddition reaction often requires the presence of catalytic amounts of nonradiolabeled Cu(I) ions, which interfere with radiometals, such as ⁶⁴Cu, and make click reaction unfavorable for the development of radiometal-labeled PET probes. With the recent discovery of Cu(I)-free 1,3-dipolar cycloaddition reactions,^{16,17} several strain-promoted systems, such as cyclooctynes and dibenzocyclooctynes, have been developed for ¹⁸F labeling,^{18,19} but few examples were reported in radiometal labeling.²⁰ One elegant study was to use a Diels–Alder reaction (norbornene-tetrazine ligation) to prepare ⁶⁴Cu-labeled antibodies.²¹ To the best of our knowledge, the catalyst-free aza-dibenzocyclooctyne ligation has not yet been employed in the radiometal-labeled probes. Herein we present a study of using aza-dibenzocyclooctyne ligation—a fast and efficient approach to synthesize ⁶⁴Cu-labeled probes. A ⁶⁴Cu-labeled derivative of cyclic RGD peptide [c(RGDfK)] (Figure 1), a well-validated integrin $\alpha_v\beta_3$

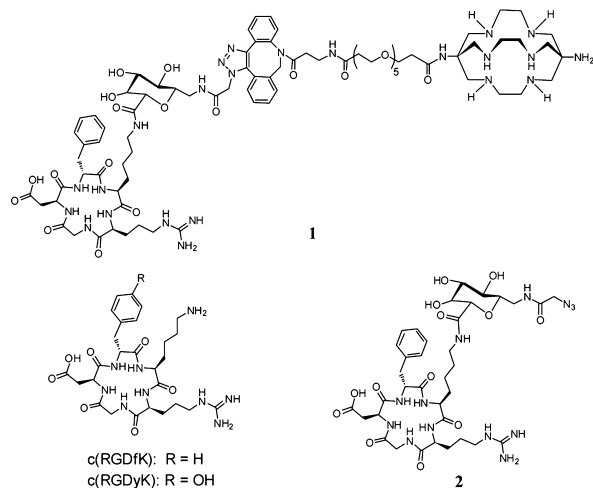


Figure 1. Chemical structures of relevant RGD peptides.

ligand,^{22–24} was exemplified by using the “click” method. We further demonstrate that our “click” RGD probe maintains good binding affinity to the integrin $\alpha_v\beta_3$ receptor and exhibits excellent tumor targeting and retention properties in an integrin $\alpha_v\beta_3$ -positive mouse tumor model.

Our starting point was to select a suitable azide moiety containing RGD peptide. It was found that glycosylation on the lysine side chain of cyclic RGD peptides decreased lipophilicity and hepatic uptake.²⁵ This finding prompted us to consider methods for preparing azido galacto-RGD peptide. To this end, we synthesized 2 as shown in Figure 1. The fully protected c[R(Pbf)GD(O^tBu)fK] peptide was conjugated with Fmoc-protected galacturonic acid derivative, followed by deprotection of the Fmoc group, azido acetic acid coupling, and deprotections of guanidine and acid (Supporting Information). The synthesis was achieved in four steps with a total yield of 44%. We successfully obtained 2 in a great chemical purity (>95%) without HPLC purification.

We next sought to select a suitable ⁶⁴Cu-chelator complex system, which can be readily conjugated with a strained alkyne. Various bifunctional chelators (BFCs), including widely used cyclam and cyclen backbones-based chelators and cross-bridged

tetraamine ligands, have been developed for ⁶⁴Cu labeling.^{8–10,26} Recently, a new class of BFCs, based on the cage-like hexaazamacrobicyclic sarcophagine, has gained great attention as potential ⁶⁴Cu chelators. We and others demonstrated that either one of the primary amines of 3,6,10,13,16,19-hexaazabicyclo[6.6.6]eicosane-1,8-diamine (DiAmSar) or both primary amines could be modified and coupled with biologically relevant ligands.^{27–29} The resulting ⁶⁴Cu complexes present improved *in vivo* stability and radiolabeling efficiency. On the other hand, an aza-dibenzocyclooctyne system has been proved to be simultaneously reactive and stable.³⁰ Therefore, we attempted to build a DiAmSar-containing dibenzocyclooctyne analog as a strained alkyne as well as a ⁶⁴Cu labeling precursor. In addition, because a poly(ethylene glycol) (PEG) linker can fine-tune the *in vivo* pharmacokinetics of imaging probes,^{31,32} we aimed to incorporate a PEG linker between DiAmSar and dibenzocyclooctyne. Our synthesis started from commercially available dibenzocyclooctyne, which was coupled with a short PEG linker. After the activation of the carboxylic acid group, the PEG-dibenzocyclooctyne was conjugated to the commercially available DiAmSar in basic sodium borate buffer to afford 3 in 45% yield (Supporting Information). Radiolabeling of 3 with ⁶⁴Cu was efficiently accomplished at 40 °C in 0.4 M NH₄OAc buffer within 30 min (Figure 2a and

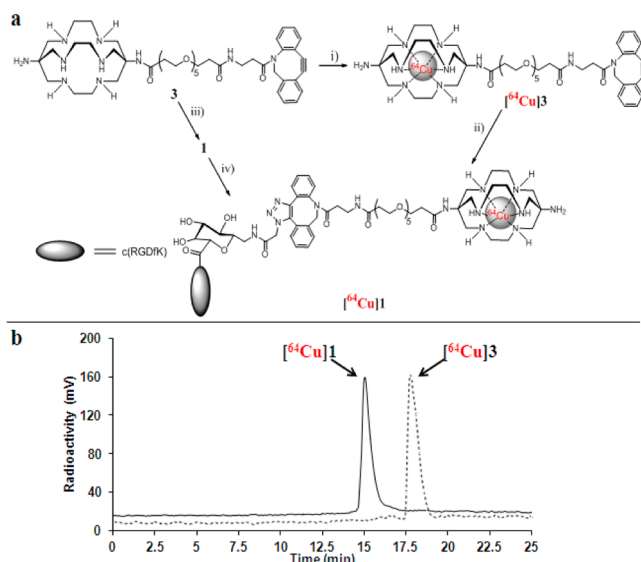


Figure 2. (a) Synthesis of [⁶⁴Cu]1. Reagents and conditions: (i) ⁶⁴CuCl₂, 40 °C, 0.4 M NH₄OAc; (ii) RGD peptide 2, 45 °C, H₂O; (iii) RGD peptide 2, room temperature, H₂O; (iv) ⁶⁴CuCl₂, 40 °C, 0.4 M NH₄OAc. (b) Radio-HPLC profiles of [⁶⁴Cu]1 and [⁶⁴Cu]3.

Supporting Information). The product [⁶⁴Cu]3 was purified by HPLC. The radioactive peak containing [⁶⁴Cu]3 appeared at 17.67 min, as shown in Figure 2b. The specific activity of [⁶⁴Cu]3 was estimated to be 37 MBq·nmol⁻¹.

To optimize the conjugation between 2 and [⁶⁴Cu]3, we systematically investigated the coupling efficiency under various reaction conditions by changing reaction factors, including reactant stoichiometry, solvent, reaction time, and reaction temperature. The conjugations between 2 and [⁶⁴Cu]3 were initially carried out in deionized water and analyzed by analytical HPLC. When [⁶⁴Cu]3 (3.7 Mbq, 1 μM) was mixed with a large excess of 2 (>100-fold) at room temperature, [⁶⁴Cu]3 was rapidly consumed within 10–15 min, and [⁶⁴Cu]1

Table 1. Optimization of Synthesis of [⁶⁴Cu]1 through the Strain-Promoted Catalyst-Free Conjugation between 2 and [⁶⁴Cu]3

entry	2 (μM)	[⁶⁴ Cu]3 ^a	solvent	temp (°C)	reaction time (min)	radiochem yield (%)
1	228	3.7 MBq (1 μM)	H ₂ O	25	15	>98
2	114	3.7 MBq (1 μM)	H ₂ O	25	10	92
3	5.7	3.7 MBq (1 μM)	H ₂ O	25	10	42
4	5.7	3.7 MBq (1 μM)	H ₂ O	45	10	>98
5	1.14	3.7 MBq (1 μM)	H ₂ O	45	15	>98
6	0.29	1.85 MBq (0.5 μM)	H ₂ O	45	10	16
7	1.14	3.7 MBq (1 μM)	PBS buffer	45	15	>98

^aThe concentration was estimated based on the specific activity of [⁶⁴Cu]3 (37 MBq·nmol⁻¹), taking into account a correction of radioactive decay.

(*t_R* = 15.05 min, Figure 2b) formed in >92% radiochemical yield (Table 1, entries 1 and 2). With a small excess of 2 (5.7-fold), the radiochemical yield was decreased to 42% after combining 2 and [⁶⁴Cu]3 for 10 min at room temperature (entry 3). However, the elevated temperature (45 °C) significantly enhanced the [⁶⁴Cu]1 yield (>98%, entry 4) after 10-min mixing of 2 and [⁶⁴Cu]3. With prolonged reaction time (15 min), an excellent radiochemical yield (>98%) of [⁶⁴Cu]1 was still achieved by using a 1.14:1 ratio of 2 and [⁶⁴Cu]3 (entry 5). Further reducing the concentration of 2 and [⁶⁴Cu]3 resulted in a low [⁶⁴Cu]1 yield (16%, entry 6). We also investigated the efficiency of the conjugation between 2 and [⁶⁴Cu]3 in phosphate buffered saline (PBS). As shown in entry 7, [⁶⁴Cu]1 was formed in a quantitative yield at 45 °C within 15 min. Among the explored reaction conditions, coupling of 2 and [⁶⁴Cu]3 with a 1.14:1 ratio at 45 °C for 15 min in deionized water or PBS buffer exhibits the highest conjugation efficiency. In addition, after coupling of 2 and [⁶⁴Cu]3, we did not observe any major side product peaks in HPLC analysis, indicating that the catalyst-free click reaction was rather clean and no free ⁶⁴Cu was released during radiolabeling.

To compare with “click” labeling of [⁶⁴Cu]1, direct labeling of 1 with ⁶⁴Cu was also conducted (Figure 2a). The conjugation of 2 and 3 was initially carried out at room temperature. As anticipated, RGD peptide 1 was formed rapidly in an excellent yield (95%) after HPLC purification (Supporting Information). Radiolabeling of 1 with ⁶⁴Cu could be achieved at 40 °C in 0.4 M NH₄OAc buffer within 30 min. The HPLC retention time (15.05 min) of product from direct ⁶⁴Cu labeling of 1 was consistent with that of “click” ⁶⁴Cu labeling product (Figure 2b), suggesting the products from two labeling methods were identical. It is also noteworthy that the specific activity of [⁶⁴Cu]1 from the direct labeling method (30–37 MBq·nmol⁻¹) was close to that from the “click” labeling approach (30 MBq·nmol⁻¹).

The *in vitro* stability of [⁶⁴Cu]1 was evaluated after 1, 6, and 24 h of incubation in PBS or mouse serum by radio-HPLC (Figure S1). Chromatographic results demonstrated no release of ⁶⁴Cu from the conjugate over a period of 24 h. This high stability is attributed to a Sar cage in the conjugate. The octanol/water partition coefficient (log *P*) for [⁶⁴Cu]1 was determined to be -1.94 ± 0.10 (Supporting Information), suggesting that [⁶⁴Cu]1 is rather hydrophilic. In addition, it is known that the U87MG human glioblastoma cell line overexpresses integrin α_vβ₃ receptor.³³ Therefore, we used the U87MG cells to measure the integrin α_vβ₃ binding affinity of 1 by a competitive cell-binding assay,³³ where ¹²⁵I-echistatin was employed as integrin α_vβ₃-specific radioligand for competitive displacement. The IC₅₀ values of c(RGDyK) and 1, which represent the concentrations required to displace 50% of the ¹²⁵I-echistatin bound to the U87MG cells, were

determined to be 105 ± 5 nM and 170 ± 3 nM, respectively (Figure S2). The slightly decreased integrin α_vβ₃ binding of 1 as compared to c(RGDyK) indicates a minimum impact of a long tail (containing galactose, triazole, and Sar moieties) on the binding of c(RGDfK) to integrin α_vβ₃ receptors.

The *in vivo* tumor-targeting efficacy of [⁶⁴Cu]1 was evaluated in nude mice bearing U87MG human glioblastoma xenograft tumors (*n* = 5) by static microPET scans at 2, 4, and 20 h after tail-vein injection of [⁶⁴Cu]1. Representative coronal slices that contained the tumor are shown in Figure 3. U87MG tumors

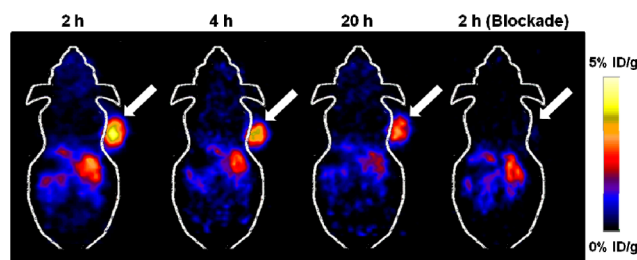


Figure 3. Decay-corrected whole-body microPET images of U87MG tumor-bearing mice (*n* = 5) at 2, 4, and 20 h after intravenous injection of [⁶⁴Cu]1. The image obtained with coinjection of c(RGDyK) (10 mg/kg body weight) is shown for a 2 h blockade (right). Tumors are indicated by arrows.

were clearly visualized at all time points examined. Region-of-interest (ROI) analysis on microPET images showed the tumor uptake values were 4.96 ± 0.73, 4.11 ± 0.54, and 2.41 ± 0.31% ID/g at 2, 4, and 20 h postinjection (pi), respectively (Table 2). At 2 h pi, the tumor/muscle, tumor/liver, and tumor/kidneys ratios reached 11.88 ± 1.31, 2.85 ± 0.28, and 2.22 ± 0.26, respectively. Consequently, the high tumor-to-normal tissue

Table 2. Decay-Corrected Biodistribution of [⁶⁴Cu]1 in U87MG Tumor-Bearing Mice Quantified by microPET Imaging (*n* = 5)^a

tissue ^b	2 h	2 h (blockade)	4 h	20 h
Percent Injected Dose/gram (% ID/g)				
T	4.96 ± 0.73	0.71 ± 0.30	4.11 ± 0.54	2.41 ± 0.31
M	0.42 ± 0.05	0.27 ± 0.04	0.36 ± 0.07	0.35 ± 0.05
L	1.76 ± 0.35	1.16 ± 0.15	1.64 ± 0.23	1.25 ± 0.23
K	2.23 ± 0.21	2.09 ± 0.28	1.79 ± 0.20	0.69 ± 0.26
Tumor-to-Normal Tissue Uptake Ratio				
T/M	11.88 ± 1.31	2.52 ± 0.81	11.65 ± 1.83	7.03 ± 1.22
T/L	2.85 ± 0.28	0.60 ± 0.22	2.51 ± 0.16	1.96 ± 0.26
T/K	2.22 ± 0.26	0.33 ± 0.11	2.32 ± 0.35	3.87 ± 1.26

^aThe results are presented as mean ± SD (*n* = 5). ^bT, tumor; M, muscle; L, liver; K, kidneys.

ratios provided excellent contrast for PET imaging. A blocking experiment was conducted to confirm the integrin $\alpha_v\beta_3$ specificity of [^{64}Cu]1. In the presence of a blocking dose (10 mg/kg) of c(RGDyK), the U87MG tumor uptake was reduced to the background level ($0.71 \pm 0.30\% \text{ID/g}$) at 2 h pi (Figure 3 and Table 2). The uptake values of normal tissues (e.g., muscle, liver, and kidneys) were also lower than those without coinjection of c(RGDyK) (Table 2). The *ex vivo* biodistribution of [^{64}Cu]1 was examined in U87MG tumor-bearing mice at 20 h pi after a microPET scan with and without coinjection of c(RGDyK) (10 mg/kg of mouse body weight). The percentage injected dose per gram of tissue (%ID/g) was shown in Figure S3. The biodistribution results were consistent with the quantitative analysis of microPET imaging. At 20 h pi, the U87MG tumor uptake of [^{64}Cu]1 reached $2.26 \pm 0.17\% \text{ID/g}$, whereas the presence of c(RGDyK) peptide significantly reduced the tumor uptake to $0.45 \pm 0.12\% \text{ID/g}$ ($P < 0.01$) in the blocking group. In addition, [^{64}Cu]1 displayed little accumulation and retention in liver and kidneys at 20 h pi. For the nonblocking group, $1.21 \pm 0.17\% \text{ID/g}$ and $0.65 \pm 0.11\% \text{ID/g}$ remained in the liver and kidneys, respectively. Furthermore, similar to microPET imaging analyses, the presence of c(RGDyK) peptide decreased the overall uptake of [^{64}Cu]1 in most tissues and organs. Based on the biodistribution results, the contrast ratios of tumor to normal organs for the nonblocking and blocking groups were calculated. For the nonblocking group, the ratio of tumor uptake to muscle, liver, and kidneys uptake at 20 h pi was calculated to be 5.65 ± 0.11 , 1.87 ± 0.17 , and 3.48 ± 0.14 , respectively, while the corresponding values for the blocking group were 1.41 ± 0.10 , 0.64 ± 0.11 , and 0.83 ± 0.13 , respectively. Overall, the biodistribution pattern of the ^{64}Cu -labeled “click” RGD probe is quite similar to what we previously obtained for ^{64}Cu -labeled non-“click” RGD probes.²⁷

In conclusion, a new catalyst-free click chemistry approach based on strain-promoted aza-dibenzocyclooctyne ligation has been developed for ^{64}Cu -labeling of biomolecules. In our new approach, we first prepared a ^{64}Cu -labeled alkyne-containing component (prosthetic group), followed by conjugation of biomolecule via click chemistry. Successful employment of catalyst-free click chemistry in the preparation of ^{64}Cu -labeled probes, which was demonstrated in our work, can eliminate the contamination problem of catalyst Cu(I) ions under the conventional Cu-catalyst 1,3-dipolar cycloaddition condition. The strain-promoted click reaction proceeds with a fast rate at low concentration, making it superior to other types of conjugation reactions for radiolabeling with short-lived isotopes, such as ^{64}Cu . Although we focused on the use of integrin $\alpha_v\beta_3$ -specific RGD peptide for proof of principle, the technique is versatile and can be applied to other ^{64}Cu -labeled or other radiometal-labeled probes. More importantly, this new catalyst-free click approach creates a modular platform in which a biomolecule can be modified with a wide variety of chelators and radiometals. Given the fact that different radiometals often require different chelators, this methodology could no doubt assist in the rapid and robust construction of highly diverse radiometalated bioconjugates for *in vitro* and *in vivo* screenings, and radioimaging and radiotherapy applications.

■ ASSOCIATED CONTENT

■ Supporting Information

Experimental procedures, cell-based integrin $\alpha_v\beta_3$ receptor binding, and biodistribution data. This material is available free of charge via the Internet at <http://pubs.acs.org>.

■ AUTHOR INFORMATION

Corresponding Authors

*Tel: 323-442-3858. Fax: 323-442-3253. E-mail: K.C., chenkai@usc.edu.

*E-mail: P.S.C., pconti@usc.edu

Present Address

2250 Alcazar Street, CSC103, Molecular Imaging Center, Department of Radiology, Keck School of Medicine, University of Southern California, Los Angeles, CA 90033, USA.

Author Contributions

[§]These authors contributed equally.

Funding Sources

This work was supported by the research fund (#IRG-58-007-51) from the American Cancer Society and by the USC Department of Radiology.

Notes

The authors declare no competing financial interest.

■ ABBREVIATIONS

PET, positron emission tomography; CT, computed tomography; HPLC, high performance liquid chromatography; DiAmSar, 3,6,10,13,16,19-hexaazabicyclo[6.6.6]eicosane-1,8-diamine; BFCs, bifunctional chelators; PEG, poly(ethylene glycol); pi, postinjection; PBS, phosphate buffered saline

■ REFERENCES

- (1) Phelps, M. E. Positron emission tomography provides molecular imaging of biological processes. *Proc. Natl. Acad. Sci. U.S.A.* **2000**, *97* (16), 9226–9233.
- (2) Gambhir, S. S. Molecular imaging of cancer with positron emission tomography. *Nat. Rev. Cancer* **2002**, *2* (9), 683–693.
- (3) Chen, K.; Conti, P. S. Target-specific delivery of peptide-based probes for PET imaging. *Adv. Drug Delivery Rev.* **2010**, *62* (11), 1005–1022.
- (4) Ametamey, S. M.; Honer, M.; Schubiger, P. A. Molecular imaging with PET. *Chem. Rev.* **2008**, *108* (5), 1501–1516.
- (5) Chen, K.; Chen, X. Positron emission tomography imaging of cancer biology: current status and future prospects. *Semin. Oncol.* **2011**, *38* (1), 70–86.
- (6) Miller, P. W.; Long, N. J.; Vilar, R.; Gee, A. D. Synthesis of ^{11}C , ^{18}F , ^{15}O , and ^{13}N radiolabels for positron emission tomography. *Angew. Chem., Int. Ed. Engl.* **2008**, *47* (47), 8998–9033.
- (7) Zeglis, B. M.; Lewis, J. S. A practical guide to the construction of radiometalated bioconjugates for positron emission tomography. *Dalton Trans.* **2011**, *40* (23), 6168–6195.
- (8) Hao, G.; Singh, A. N.; Oz, O. K.; Sun, X. Recent advances in copper radiopharmaceuticals. *Curr. Radiopharm.* **2011**, *4* (2), 109–121.
- (9) Ma, M. T.; Donnelly, P. S. Peptide targeted copper-64 radiopharmaceuticals. *Curr. Top. Med. Chem.* **2011**, *11* (5), 500–520.
- (10) Shokeen, M.; Anderson, C. J. Molecular imaging of cancer with copper-64 radiopharmaceuticals and positron emission tomography (PET). *Acc. Chem. Res.* **2009**, *42* (7), 832–841.
- (11) Kolb, H. C.; Sharpless, K. B. The growing impact of click chemistry on drug discovery. *Drug Discovery Today* **2003**, *8* (24), 1128–1137.

- (12) Carlmark, A.; Hawker, C.; Hult, A.; Malkoch, M. New methodologies in the construction of dendritic materials. *Chem. Soc. Rev.* **2009**, *38* (2), 352–362.
- (13) Lallana, E.; Riguera, R.; Fernandez-Megia, E. Reliable and efficient procedures for the conjugation of biomolecules through Huisgen azide-alkyne cycloadditions. *Angew. Chem., Int. Ed. Engl.* **2011**, *50* (38), 8794–8804.
- (14) Lutz, J. F.; Zarafshani, Z. Efficient construction of therapeutics, bioconjugates, biomaterials and bioactive surfaces using azide-alkyne “click” chemistry. *Adv. Drug Delivery Rev.* **2008**, *60* (9), 958–970.
- (15) Nwe, K.; Brechbiel, M. W. Growing applications of “click chemistry” for bioconjugation in contemporary biomedical research. *Cancer Biother. Radiopharm.* **2009**, *24* (3), 289–302.
- (16) Debets, M. F.; van Berkel, S. S.; Dommerholt, J.; Dirks, A. T.; Rutjes, F. P.; van Delft, F. L. Bioconjugation with strained alkenes and alkynes. *Acc. Chem. Res.* **2011**, *44* (9), 805–815.
- (17) Jewett, J. C.; Bertozzi, C. R. Cu-free click cycloaddition reactions in chemical biology. *Chem. Soc. Rev.* **2010**, *39* (4), 1272–1279.
- (18) Campbell-Verduyn, L. S.; Mirfeizi, L.; Schoonen, A. K.; Dierckx, R. A.; Elsinga, P. H.; Feringa, B. L. Strain-promoted copper-free “click” chemistry for ^{18}F radiolabeling of bombesin. *Angew. Chem., Int. Ed. Engl.* **2011**, *50* (47), 11117–11120.
- (19) Li, Z.; Cai, H.; Hassink, M.; Blackman, M. L.; Brown, R. C.; Conti, P. S.; Fox, J. M. Tetrazine-trans-cyclooctene ligation for the rapid construction of ^{18}F labeled probes. *Chem. Commun.* **2010**, *46* (42), 8043–8045.
- (20) Baumhover, N. J.; Martin, M. E.; Parameswarappa, S. G.; Klopping, K. C.; O’Dorisio, M. S.; Pigge, F. C.; Schultz, M. K. Improved synthesis and biological evaluation of chelator-modified alpha-MSH analogs prepared by copper-free click chemistry. *Bioorg. Med. Chem. Lett.* **2011**, *21* (19), 5757–5761.
- (21) Zeglis, B. M.; Mohindra, P.; Weissmann, G. I.; Divilov, V.; Hilderbrand, S. A.; Weissleder, R.; Lewis, J. S. Modular strategy for the construction of radiometalated antibodies for positron emission tomography based on inverse electron demand Diels-Alder click chemistry. *Bioconjugate Chem.* **2011**, *22* (10), 2048–2059.
- (22) Cai, W.; Chen, X. Multimodality molecular imaging of tumor angiogenesis. *J. Nucl. Med.* **2008**, *49* (Suppl 2), 113S–128S.
- (23) Haubner, R.; Beer, A. J.; Wang, H.; Chen, X. Positron emission tomography tracers for imaging angiogenesis. *Eur. J. Nucl. Med. Mol. Imaging* **2010**, *37* (Suppl 1), S86–103.
- (24) Liu, S. Radiolabeled multimeric cyclic RGD peptides as integrin $\alpha_v\beta_3$ targeted radiotracers for tumor imaging. *Mol. Pharmaceutics* **2006**, *3* (5), 472–487.
- (25) Haubner, R.; Wester, H. J.; Burkhart, F.; Senekowitsch-Schmidtke, R.; Weber, W.; Goodman, S. L.; Kessler, H.; Schwaiger, M. Glycosylated RGD-containing peptides: tracer for tumor targeting and angiogenesis imaging with improved biokinetics. *J. Nucl. Med.* **2001**, *42* (2), 326–336.
- (26) Chen, K.; Sun, X.; Niu, G.; Ma, Y.; Yap, L. P.; Hui, X.; Wu, K.; Fan, D.; Conti, P. S.; Chen, X. Evaluation of ^{64}Cu labeled GX1: A phage display peptide probe for PET imaging of tumor vasculature. *Mol. Imaging Biol.* **2012**, *14* (1), 96–105.
- (27) Cai, H.; Li, Z.; Huang, C. W.; Shahinian, A. H.; Wang, H.; Park, R.; Conti, P. S. Evaluation of copper-64 labeled AmBaSar conjugated cyclic RGD peptide for improved microPET imaging of integrin $\alpha_v\beta_3$ expression. *Bioconjugate Chem.* **2010**, *21* (8), 1417–1424.
- (28) Liu, S.; Li, Z.; Yap, L. P.; Huang, C. W.; Park, R.; Conti, P. S. Efficient preparation and biological evaluation of a novel multivalency bifunctional chelator for ^{64}Cu radiopharmaceuticals. *Chemistry* **2011**, *17* (37), 10222–10225.
- (29) Ma, M. T.; Neels, O. C.; Denoyer, D.; Roselt, P.; Karas, J. A.; Scanlon, D. B.; White, J. M.; Hicks, R. J.; Donnelly, P. S. Gallium-68 complex of a macrobicyclic cage amine chelator tethered to two integrin-targeting peptides for diagnostic tumor imaging. *Bioconjugate Chem.* **2011**, *22* (10), 2093–2103.
- (30) Debets, M. F.; van Berkel, S. S.; Schoffelen, S.; Rutjes, F. P.; van Hest, J. C.; van Delft, F. L. Aza-dibenzocyclooctynes for fast and efficient enzyme PEGylation via copper-free (3 + 2) cycloaddition. *Chem. Commun.* **2010**, *46* (1), 97–99.
- (31) Chen, X.; Hou, Y.; Tohme, M.; Park, R.; Khankaldyyan, V.; Gonzales-Gomez, I.; Bading, J. R.; Laug, W. E.; Conti, P. S. Pegylated Arg-Gly-Asp peptide: ^{64}Cu labeling and PET imaging of brain tumor $\alpha_v\beta_3$ -integrin expression. *J. Nucl. Med.* **2004**, *45* (10), 1776–1783.
- (32) Wu, Z.; Li, Z. B.; Cai, W.; He, L.; Chin, F. T.; Li, F.; Chen, X. ^{18}F -labeled mini-PEG spacers RGD dimer (^{18}F -FPRGD2): synthesis and microPET imaging of $\alpha_v\beta_3$ integrin expression. *Eur. J. Nucl. Med. Mol. Imaging* **2007**, *34* (11), 1823–1831.
- (33) Zhang, X.; Xiong, Z.; Wu, Y.; Cai, W.; Tseng, J. R.; Gambhir, S. S.; Chen, X. Quantitative PET imaging of tumor integrin $\alpha_v\beta_3$ expression with ^{18}F -FRGD2. *J. Nucl. Med.* **2006**, *47* (1), 113–121.